

$\pi^-/\pi^+$  Ratio for Photoproduction from Deuterium\*

J. PINE† AND M. BAZIN‡

*High-Energy Physics Laboratory, Stanford University, Stanford, California*

(Received 20 June 1963)

The ratio of the  $\pi^-$  and  $\pi^+$  photoproduction cross sections from deuterium has been measured for 12 combinations of pion angle and momentum. In terms of the kinematics for  $\gamma + p \rightarrow \pi^+ + n$ , the experiment covers photon energies from 165 to 200 MeV and center-of-mass angles from 40 to 145°. The results are corrected to obtain the  $\pi^-/\pi^+$  ratio for free nucleons, and, from comparison with theory, the  $\gamma\pi\rho$  coupling constant  $\Lambda$  is estimated to be  $+0.1 \pm 0.3$ .

## INTRODUCTION

COMPARISON of the cross sections for the reactions  $\gamma + n \rightarrow \pi^- + p$  and  $\gamma + p \rightarrow \pi^+ + n$  is of particular interest because their ratio,  $R$ , is mainly sensitive to the isoscalar photoproduction amplitude. In the notation of CGLN,<sup>1</sup>

$$R = |\mathcal{F}^- - \mathcal{F}^0|^2 / |\mathcal{F}^- + \mathcal{F}^0|^2,$$

where the isovector amplitude  $\mathcal{F}^-$  dominates the isoscalar amplitude  $\mathcal{F}^0$ , so that  $R$  is  $\sim 1$  but is much more sensitive to variation of  $\mathcal{F}^0$  than to variation of  $\mathcal{F}^-$ . Several authors<sup>2-4</sup> have pointed out that  $\mathcal{F}^0$  is affected by the  $\pi\pi$  interaction in the  $T=J=1$  state (the  $\rho$  meson) and emphasized the usefulness of studies of  $R$  in this connection.

The reaction  $\gamma + n \rightarrow \pi^- + p$  can be studied by using target neutrons bound in nuclei or by measuring the inverse reaction. While the latter method is quite free of complications, it is experimentally very difficult and has just recently been attempted.<sup>5</sup> Photoproduction from deuterium has long been used to obtain information about  $R$ , although various corrections to the experimentally determined ratio  $R_d$  ( $\pi^-/\pi^+$  ratio from deuterium) are necessary. Instead of determining  $R_d$ , it is also possible to study the reaction  $\gamma + D \rightarrow \pi^- + p + p$  and to observe all three particles in the final state. From these data, with corrections for both Coulomb and nuclear effects, the cross section for  $\gamma + n \rightarrow \pi^- + p$  can be inferred.<sup>6</sup> Hogg has recently summarized the available experimental data for  $R$ .<sup>7</sup>

The measurements reported here determine  $R_d$  with improved accuracy for laboratory pion momenta of 59 to 98 MeV/c. For pions at a given angle and momentum a nominal gamma ray energy is specified by the two-body kinematics for  $\pi^+$  photoproduction from protons. With the pion momentum range noted above, a full angular distribution for  $R_d$  has been determined for 180-MeV photons, with more limited data at 165, 170, and 200 MeV. These energies are high enough to keep the corrections due to final-state interactions relatively small, and low enough to simplify the theoretical interpretation.

## APPARATUS

A plan view of the experimental arrangement is shown in Fig. 1(a). The electron beam of the Stanford Mark III linear accelerator (with energy set at 1.25 times the photon energy of interest) was incident on a tantalum radiator 0.05 radiation-length thick. The sweeping magnet deflected positrons and electrons from the radiator in a vertical plane, and the gamma-ray beam struck a liquid deuterium target. The target cell

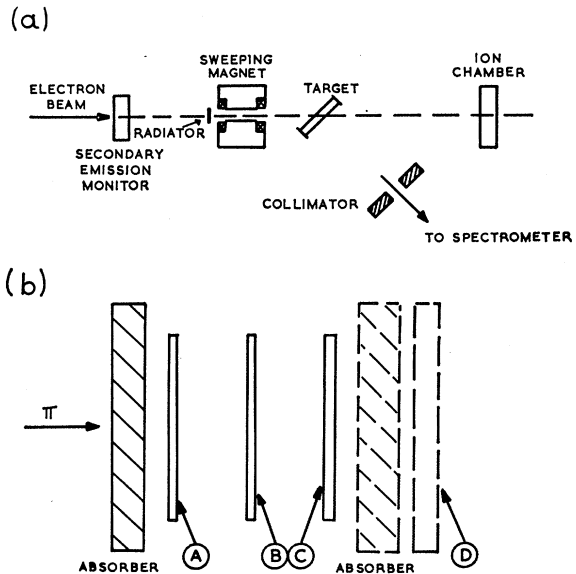


FIG. 1. (a) Plan view of the experimental layout. (b) Scintillation counter telescope and Polystyrene absorbers. Counter D and the second absorber are used only for studies of the muon and electron background.

\* Supported by the joint program of the Atomic Energy Commission, the Office of Naval Research, and the Air Force Office of Scientific Research.

† Present address: Physics Department, California Institute of Technology, Pasadena.

‡ Present address: Laboratoire de Physique, Ecole Polytechnique, Paris, France.

<sup>1</sup> G. F. Chew, M. Goldberger, G. Low, and Y. Nambu, *Phys. Rev.* **106**, 1345 (1957).

<sup>2</sup> J. S. Ball, *Phys. Rev.* **124**, 2014 (1961).

<sup>3</sup> M. Gourdin, D. Lurié, and A. Martin, *Nuovo Cimento* **18**, 933 (1960).

<sup>4</sup> B. De Tollis, E. Ferrari, and H. Munczek, *Nuovo Cimento* **18**, 198 (1960).

<sup>5</sup> G. Gatti, P. Hillman, W. C. Middelkoop, T. Yamagata, and E. Zavattini, CERN Report 61-28, 1961 (unpublished).

<sup>6</sup> M. I. Adamovich, G. V. Kuzmicheva, V. G. Larionova, and S. P. Kharlamov, *Zh. Ekeperim. i Teor. Fiz.* **35**, 27 (1958) [translation: *Soviet Phys.—JETP* **8**, 21 (1959)].

<sup>7</sup> W. R. Hogg, *Proc. Phys. Soc. (London)* **80**, 729 (1962).

was a horizontal duralumin cylinder, 6 in. long,  $\frac{3}{4}$  in. in diam, with 0.003 in. walls. Since the long axis of the cylinder was kept at  $45^\circ$  to the beam, mesons at angles  $\leq 90^\circ$  were detected with the spectrometer to the right of the beam, and mesons at angles  $\geq 90^\circ$  were detected with the spectrometer to the left.

The beam current was measured and integrated with two monitors used simultaneously. A secondary emission monitor in front of the radiator recorded the electron-beam current, while a hydrogen-ion chamber behind the target measured the gamma-ray intensity. The integrated currents from the two monitors were in a constant ratio to within  $\pm 0.2\%$  during every determination of  $R_d$ .

The double-focusing "zero-dispersion" spectrometer has been described elsewhere.<sup>8,9</sup> A lead collimator 10 in. from the target, with an aperture  $1\frac{1}{2}$  in. high and 2 in. wide, was used to minimize the flux of electrons and positrons scattered into the spectrometer from various parts of the target vacuum chamber. The momentum spread,  $\Delta p/p$ , accepted by the spectrometer was varied from 4% at the lowest pion momenta to 2% at the highest momenta, so that the pion range spread was kept small. The magnetic field of the spectrometer was set with a rotating coil flux meter, with an accuracy of better than 0.1%.

Pions were detected at the focus of the spectrometer with the scintillation counter telescope shown in Fig. 1(b). Normally, the telescope consisted of counters A, B, and C in coincidence, preceded by a Polystyrene absorber. For counting pions, the absorber thickness was set so that pions just passed through the telescope, emerging with approximately 7-MeV kinetic energy. For subtracting the background of muons and electrons, the absorber thickness was increased to stop the pions but permit the muons and electrons to traverse the telescope. In view of the asymmetry in the behavior of stopped  $\pi^+$  and  $\pi^-$  mesons, the pion detection did not utilize a range telescope based on coincidence and anti-coincidence requirements. Pions stopped in the wall of the "counter house," approximately 2 ft behind the telescope, and the pulse-height distributions in all counters were observed to be identical for  $\pi^+$  and  $\pi^-$ . For the muon and electron subtraction, the pions were stopped sufficiently deep within the absorber so that, again, no asymmetry was observed in the pulse-height distributions.

Counter D and the absorber between C and D were used only in side experiments to study the relative proportions of muons and electrons in the background, and to study the variation as a function of front absorber thickness of the efficiency of muons in producing ABC coincidences. For these measurements counter, D was the anticoincidence counter of a range telescope.

Counters A, B, and C were 3 in. square, with thick-

nesses 0.062 in., 0.062 in., and 0.100 in., while D was 4 in.  $\times$  4 in.  $\times$   $\frac{3}{8}$  in. The electronics, as well as counters A, B, and D were the same as in the  $\pi^+$  photoproduction experiment of Ref. 9.

The counter biases were set to count pions very conservatively, with efficiency essentially 100%. The muon efficiency varied from about 50 to 100%, with the absorber set for counting pions. The electron efficiency was  $\leq 10^{-3}$ , as a result of three consecutive  $dE/dx$  requirements, and the background arising from particles penetrating the spectrometer shielding was always  $\leq 1\%$  of the pion rate.

The fact that the muon and electron background was subtracted by increasing the absorber thickness introduces a complication, since the ABC coincidence efficiencies can be expected to change. For the muons, the pulse heights increase, while for the electrons the probability of an associated secondary is increased. The variation of electron efficiency was easily studied by reducing the beam energy to below the photoproduction threshold and turning off the sweeping magnet. Electrons scattered from the target were counted at high rates in spite of the low efficiency.

The range telescope was used with counter D biased for 100% electron efficiency under the following conditions: pions stopped in the second absorber, with the front absorber at the normal value for pion ABC coincidences; and muons stopped in the second absorber, with the front absorber set for the muon and electron subtraction. The (ABC) and (ABC-D) rates were recorded simultaneously. For the first condition, (ABC)-(ABC-D) gives the muon-electron rate with thin front absorber. For the second condition (ABC) gives the muon-electron rate with thick front absorber, while (ABC)-(ABC-D) gives the electron rate. From these data, and the known change in electron efficiency, the change in muon efficiency can be found. The relative proportions of muons and electrons in the background is also determined. As was expected,  $\pi^-$  stars sometimes caused trouble in the first condition, but the variation of muon efficiency could be satisfactorily determined from measurements with positive muons. The results of these studies will be discussed in the following section.

## DATA, CORRECTIONS, AND UNCERTAINTIES

### Experimental

A sequence of data consisted of measurements of full and empty target yields with both thin and thick absorbers. Each yield was measured for  $\pi^-$  and  $\pi^+$  mesons by frequent alternation of the spectrometer field direction. For either pion charge, the four rates, being full target, thin absorber; full target, thick absorber; empty target, thin absorber; empty target, thick absorber; were typically in the ratios 100:10:10:1. The absorber could be quickly changed, and the target quickly emptied and refilled by transferring the liquid

<sup>8</sup> R. Alvarez, K. Brown, W. Panofsky, and C. Rockhold, Rev. Sci. Instr. **31**, 556 (1960).

<sup>9</sup> M. J. Bazin and J. Pine, Phys. Rev. **132**, 830 (1963).

TABLE I. Results and corrections.  $R_d$  is the measured  $\pi^-/\pi^+$  ratio from deuterium,  $\epsilon_{\mu e}$  is an estimate of the uncertainty arising from the background subtraction,  $\delta_\gamma$  is the correction for the threshold difference for  $\pi^-$  and  $\pi^+$  photoproduction,  $\delta_p$  and  $\delta_\pi$  are Coulomb corrections discussed in the text.  $R$  is the free nucleon  $\pi^-/\pi^+$  ratio, after the corrections  $\delta_\gamma$ ,  $\delta_p$ , and  $\delta_\pi$ , with purely statistical errors.

$k$ (MeV)	$\theta^*$ (deg)	$R_d$	$\epsilon_{\mu e}$ (%)	$\delta_\gamma$ (%)	$\delta_p$ (%)	$\delta_\pi$ (%)	$R$
165	65	$1.41 \pm 0.07$	$\pm 1.7$	-1.8	+4.4	-4.2	$1.39 \pm 0.07$
170	40	$1.30 \pm 0.06$	$\pm 0.3$	-1.8	+6.6	-2.5	$1.33 \pm 0.06$
170	65	$1.37 \pm 0.05$	$\pm 1.0$	-1.8	+4.5	-2.8	$1.37 \pm 0.05$
170	90	$1.37 \pm 0.08$	$\pm 1.8$	-1.8	+3.0	-3.3	$1.34 \pm 0.08$
180	40	$1.25 \pm 0.04$	$\pm 0.3$	-1.7	+6.5	-1.8	$1.29 \pm 0.04$
180	60	$1.31 \pm 0.05$	$\pm 0.3$	-1.7	+4.5	-1.9	$1.32 \pm 0.05$
180	90	$1.30 \pm 0.04$	$\pm 1.0$	-1.7	+2.6	-2.2	$1.28 \pm 0.04$
180	105	$1.40 \pm 0.05$	$\pm 0.9$	-1.7	+2.0	-2.3	$1.37 \pm 0.05$
180	135	$1.54 \pm 0.08$	$\pm 1.4$	-1.7	+1.4	-2.7	$1.49 \pm 0.08$
180	145	$1.62 \pm 0.13$	$\pm 2.0$	-1.7	+1.3	-2.8	$1.57 \pm 0.13$
200	110	$1.34 \pm 0.04$	$\pm 0.6$	-1.5	+1.3	-1.5	$1.32 \pm 0.04$
200	145	$1.60 \pm 0.05$	$\pm 0.9$	-1.5	+0.6	-1.7	$1.56 \pm 0.05$

deuterium to and from an auxiliary storage cell. As a result, data were accumulated by rapid cycling among the various yields, and the sensitivity to instrumental changes was minimized.

Each determination of  $R$  is based on two or more sequences of data, with the exception of the point at 180 MeV, 145°. (Angles will always be given in the center of mass, and photon energies in the laboratory, assuming  $\gamma + p \rightarrow \pi^+ + n$  kinematics.) At this point, the pion laboratory momentum was too low to permit the use of counter C, and it was not felt worthwhile to pursue the measurements to high statistical accuracy. The observed differences between repeated determinations of  $R_d$  at identical kinematic conditions were consistent with statistical fluctuations.

Table I summarizes the experimental results.  $R_d$  represents the measured  $\pi^-/\pi^+$  ratio from deuterium, with purely statistical errors. The muon-electron background has been subtracted at face value. The quantity  $\epsilon_{\mu e}$  is equal to  $(0.1)(\mu e)/(\pi\mu e)$ , where  $(\mu e)$  is the background rate and  $(\pi\mu e)$  is the rate with the absorber set for counting pions, with empty target rates subtracted. Defined this way,  $\epsilon_{\mu e}$  represents a conservative estimate of the uncertainty coming from the background subtraction, and conveniently shows the magnitude of the subtraction at the various experimental points.

The estimate of  $\epsilon_{\mu e}$  is based on the following considerations: The electron and positron rates were in general  $\leq 1\%$  of  $(\pi\mu e)$ , and  $4\%$  in the worst case. The electron/positron ratio was in every case consistent with unity, with the measured electron-positron difference always  $\leq 2\%$  of  $(\pi\mu e)$ . The electron efficiency with the  $(\mu e)$  absorber varied over the range of the experiment from 1.1 to 1.6 times the efficiency with the  $(\pi\mu e)$  absorber. Thus, the error in  $R_d$  from the electron background subtraction was always  $\leq 1\%$  and was neglected. In estimating the error arising from the background subtraction, we will now ascribe the rate  $(\mu e)$  entirely to muons.

The muon efficiency with the thick absorber varied

from 1.0 to 2.0 times the efficiency with the  $(\pi\mu e)$  absorber, where the range includes rather large statistical errors in the determination of the efficiency changes. The worst change, by a factor 2.0, refers to the lowest momentum, where the subtraction is largest. The  $\pi\text{-}\mu$  decay kinematics and the geometry of the experiment are such that muons entering the spectrometer mainly come from decays of pions moving toward the spectrometer. From the range of pion energies involved, and the energy dependence of  $R$ , we conservatively estimate the relationship between  $-/+$  ratios for pions and muons to be  $(\mu^-/\mu^+) = (1.0 \pm 0.2)(\pi^-/\pi^+)$ . This leads, for the worst muon efficiency change, to the value  $\epsilon_{\mu e} = (0.1) \times (\mu e)/(\pi\mu e)$ , which is listed in Table I. At higher momenta the efficiency changes by less than a factor of 2, and this becomes an overestimate. However, the subtraction is then so small that the error estimated in this way is completely negligible. Even in the worst cases,  $\epsilon_{\mu e}$  does not significantly change the statistical error, and doubling  $\epsilon_{\mu e}$  would hardly affect the results. The measured ratios  $(\mu e)^-/(\mu e)^+$  were equal to  $(\pi\mu e)^-/(\pi\mu e)^+$ , within statistical uncertainties, for every experimental point, which tends to support the arguments above.

Another error in  $R_d$  may arise from different losses of  $\pi^-$  and  $\pi^+$  mesons in the polystyrene absorber. From the results given by Stork,<sup>10</sup> the  $\pi^+$  attenuation in the absorber, from nuclear interactions and scattering, is estimated at  $\leq 2\%$  for the worst case (highest pion momentum). Since the  $\pi^-$  interaction cross section is quite similar to the  $\pi^+$  cross section, the error in  $R_d$  is estimated to be negligible.

Finally, we assume the  $\pi^-$  and  $\pi^+$  lifetimes to be equal. For the range of pion momenta involved here, between 70 and 90% of the pions decay along the 6.6 m flight path between target and counters. Thus, a 1% lifetime difference would lead to about a 2% error in  $R_d$  for the lowest pion momenta.

<sup>10</sup> D. Stork, Phys. Rev. **93**, 868 (1954).

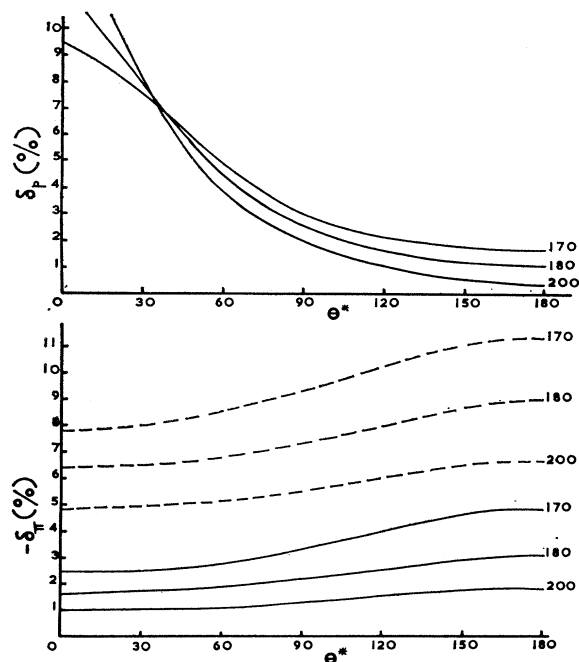


FIG. 2. The Coulomb corrections, calculated from Eqs. (3), (4), and (6).

### Threshold Correction

Owing to the neutron-proton mass difference, the threshold for  $\pi^-$  photoproduction is 2.6 MeV lower than for  $\pi^+$  photoproduction. In order to keep the ratio  $R$  free of gross effects at low energies, we should compare the reactions at identical pion kinetic energies. The technique used here does in fact do this. However, at a given pion kinetic energy the gamma-ray is 2.6 MeV lower for  $\pi^-$  photoproduction. For the gamma-ray spectrum of this experiment, this results in 1.7% higher photon intensity per incident electron for  $\pi^-$  production at 180-MeV photon energy. The correction  $\delta_\gamma$ , shown in Table I, has been applied to  $R_d$  to correct for this effect. The uncertainty in  $\delta_\gamma$  is negligible. Kharlamov *et al.*<sup>11</sup> have discussed this correction in some detail and applied it to some previous measurements of  $R_d$ .

### Coulomb Corrections

The major obstacle in accurately determining  $R$  from  $R_d$  is the asymmetry in the Coulomb interactions for the final states  $\pi^+ + n + n$  and  $\pi^- + p + p$ . By charge symmetry, the purely nuclear effects are expected to be identical. Baldin<sup>12</sup> has made a detailed calculation of both Coulomb and nuclear effects for the reaction  $\gamma + D \rightarrow \pi^- + p + p$ , with the aim of extracting the free

neutron cross section from data for the deuterium reaction with all three final particles observed. Here, where only the pion is detected, we require an average of the Baldin Coulomb corrections. In order to estimate this average we have adopted an extreme impulse approximation, in which the final state consists of one proton (the "spectator") at rest in the laboratory, plus a recoil proton and  $\pi^-$  meson with two-body photoproduction kinematics. Following Baldin, we consider separately the  $p$ - $p$  Coulomb effect and the  $\pi^-$ -( $pp$ ) Coulomb effect.  $R$  will be given by

$$R = R_d(1 + \delta_p)(1 + \delta_\pi), \quad (2)$$

where  $\delta_p$  and  $\delta_\pi$  refer to the two Coulomb corrections.

The Baldin calculation for the final-state kinematics assumed above, gives

$$(1 + \delta_p)^{-1} \cong [2\pi\eta / \exp(2\pi\eta) - 1] \times [1 + 2\eta \tan^{-1}(P/\alpha_d)], \quad (3)$$

where  $\eta = \alpha/\beta_p$ , with  $\alpha$  the fine structure constant and  $\beta_p$  equal to  $1/c$  times the recoil proton velocity;  $P$  is the momentum of the recoil proton; and  $\alpha_d$  is the deuteron wave function radial parameter, taken equal to 0.31  $m_\pi c$ . Equation (3) is an approximation, based on neglecting the  $p$ - $p$  nuclear final-state interaction in calculating the Coulomb effect. This should introduce a small error for the range of proton momenta of interest here, and greatly simplifies the formula. Values calculated from Eq. (3) are consistent with those given by Baldin for the proton kinematics of our model. The values of  $\delta_p$  for the experimental points are listed in Table I, while Fig. 2 shows the variation of  $\delta_p$  with angle and energy.

The formula for  $\delta_\pi$  given by Baldin, for the kinematics defined by our model, is

$$\delta_\pi = (-2\pi\alpha / |\mathbf{q}/m_\pi c - \mathbf{P}/2Mc|), \quad (4)$$

where  $\mathbf{q}$  is the pion momentum,  $\mathbf{P}$  is the recoil proton momentum, and  $M$  is the proton mass. However, as Baldin has pointed out, this expression is valid only when the wavelength of the meson in the diproton system is large compared with the size of the system, i.e., for  $|\mathbf{q} - \mathbf{P}/2(M/m_\pi)| \ll \alpha_d$ . In fact, for this experiment  $|\mathbf{q} - \mathbf{P}/2(M/m_\pi)|$  is always greater than  $\alpha_d$ , and Eq. (4) overestimates the correction. The dashed curves of Fig. 2 show  $\delta_\pi$  as computed from Eq. (4). (A correction of 15% corresponds to  $|\mathbf{q} - \mathbf{P}/2(M/m_\pi)| = \alpha_d$ .)

In order to make a more realistic estimate for  $\delta_\pi$  we have been guided by the form of Eq. (3). For  $\eta$  small this equation may be written

$$\delta_p \cong \pi\eta [1 - 2/\pi \tan^{-1}(P/\alpha_d)]. \quad (5)$$

If  $P \ll \alpha_d$ , then  $\delta_p \cong \pi\eta$ , which is analogous to the Coulomb correction in beta decay and to Eq. (4). The factor in square brackets reduces this correction for  $P/\alpha_d \gtrsim 1$ , thus taking account of the finite size of the

<sup>11</sup> S. P. Kharlamov, M. I. Adamovich, and V. G. Larionova, Zh. Eksperim. i Teor. Fiz. **36**, 945 (1959) [translation: Soviet Phys.—JETP **9**, 668 (1959)].

<sup>12</sup> A. Baldin, Nuovo Cimento **8**, 569 (1958).

system. We have modified Eq. (4) so that it resembles Eq. (5).

$$\delta_\pi = \frac{2\pi\alpha}{|q/m_\pi c - P/2Mc|} \times \left[ 1 - \frac{2}{\pi} \tan^{-1} \left( \frac{|q - P/2(M/m_\pi)|}{\alpha_d} \right) \right]. \quad (6)$$

While we hardly believe that this equation would result from a really correct treatment of the problem, we believe it to be closer to the truth than either assuming the correction to be negligibly small or taking Eq. (4) at face value. Values of  $\delta_\pi$ , calculated from Eq. (6), are given in Table I, and Fig. 2 shows how this correction depends on angle and energy.

The final values of  $R$  are listed in the last column of Table I, with purely statistical errors. The only other significant uncertainties arise from the Coulomb corrections and affect  $R$  systematically. We estimate the uncertainty in  $\delta_p$  to be about  $\frac{1}{3}$  the correction, while  $\delta_\pi$  is estimated to be correct to within a factor of 2. The uncertainty in  $\delta_p$  significantly affects the data only at

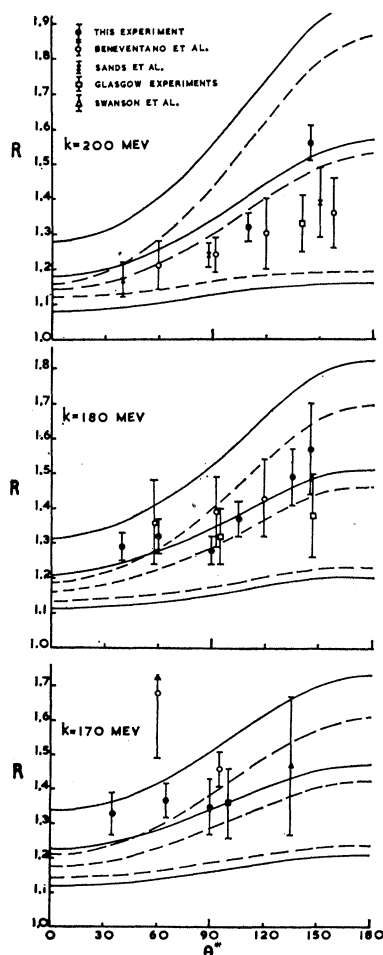
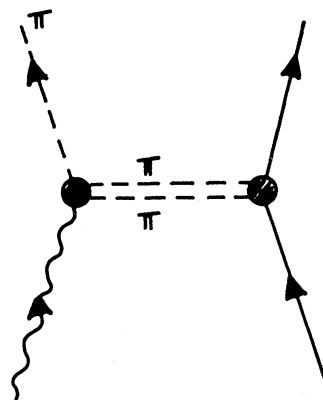


FIG. 3. The  $\pi^-/\pi^+$  ratio,  $R$ , for free nucleons, derived from this experiment and from the data of Beneventano *et al.* (see Ref. 13), Sands *et al.* (see Ref. 16), three Glasgow University experiments (see Refs. 7, 14, and 15) and Swanson *et al.* (see Ref. 17). The dashed curves are calculated from the McKinley theory for  $\Delta = -0.5, 0$ , and  $+0.5$  (top, middle, and bottom curves, respectively, at each energy). The solid curves include the corrections calculated by Warburton and Gourdin.

FIG. 4. Feynman diagram for the contribution of the  $\pi$ - $\pi$  interaction.



forward angles, while the uncertainty in  $\delta_\pi$  leads mainly to an angle-independent systematic error which varies with gamma-ray energy.

## DISCUSSION

The data for  $R$ , corrected for Coulomb effects and the threshold difference, are shown in Fig. 3. Results of other experiments<sup>7,13-17</sup> in this energy region have also been included to supplement our results and to show the consistency between various experiments. The Coulomb corrections have been computed for the other experiments as for this one. The same values of  $\delta_\gamma$  have also been applied, since they are closely correct for all the experiments. The data of Beneventano *et al.*<sup>13</sup> at 190, 200, and 210 MeV have been averaged and shown at 200 MeV. The Glasgow results<sup>7,14,17</sup> have in one case been combined, and refer to energies slightly different from those chosen here. The only major inconsistency appears to be between this experiment and others for  $\theta \geq 140^\circ$  at 200 MeV.

The dashed curves of Fig. 3 are calculated from the one dimensional dispersion relations of McKinley.<sup>18,19</sup> His formulation avoids a number of approximations used previously, and he has taken the scattering phase shifts from new empirical fits to the experimental data. The calculated curves utilize his phase-shift set "Y."

The  $\pi$ - $\pi$  interaction contributes to the isoscalar amplitude through the diagram shown in Fig. 4. Dispersion relation calculations of its effect have been made,<sup>2,3</sup> as well as calculations in the "bipion" approximation.<sup>3,4</sup>

<sup>13</sup> M. Beneventano, G. Bernardini, G. Stoppini, and L. Tau, *Nuovo Cimento* **10**, 1109 (1958).

<sup>14</sup> W. R. Hogg and E. H. Bellamy, *Proc. Phys. Soc. (London)* **72**, 895 (1958).

<sup>15</sup> J. G. Rutherglen and J. K. Walker, *Proc. Phys. Soc. (London)* **76**, 430 (1960).

<sup>16</sup> M. Sands, J. G. Teasdale, and R. L. Walker, *Phys. Rev.* **95**, 592 (1954).

<sup>17</sup> W. P. Swanson, D. C. Gates, T. L. Jenkins, and R. W. Kenney, *Phys. Rev. Letters* **5**, 336 (1960).

<sup>18</sup> J. M. McKinley, Physics Department, University of Illinois, Tech. Rept. No. 38, 1962 (unpublished).

<sup>19</sup> F. F. Liu (private communication). The curves shown here are from Liu's evaluations of McKinley formulas.

In the latter case the two pions exchanged with the nucleon are assumed to be a single particle with  $I=J=1$  ( $\rho$  meson), and a perturbation theory calculation is made. In either case results similar in form are obtained and the contribution to the isoscalar amplitude is proportional to  $\Lambda ef$ , where  $e^2=1/137$ ,  $f^2=0.08$ , and  $\Lambda$  has a value which depends on the unknown strength of the  $\gamma-3\pi$  coupling.

The calculations from the McKinley theory include the "bipion" amplitude as given by De Tollis, Ferrari, and Munczek<sup>4</sup> with the square of the bipion mass,  $t_r$ , taken as  $22.4 m_\pi^2$ . At each energy in Fig. 3, the upper dashed curve is for  $\Lambda=-0.5$ , the middle curve for  $\Lambda=0$  and the lower one for  $\Lambda=+0.5$ .

Warburton and Gourdin<sup>20</sup> have pointed out that the sensitivity of  $R$  to small changes in the isoscalar amplitude makes it necessary to consider contributions to this amplitude which have generally been neglected. They have investigated the effect of the  $I=J=\frac{1}{2}$  pion-nucleon interaction and determined the correction to  $R$  at  $90^\circ$  c.m. To a good approximation, the correction is independent of angle, and the solid curves of Fig. 3 show the McKinley theory corrected according to the results of Warburton and Gourdin. The correction consists of one contribution independent of the  $\rho$ -meson diagram, plus a  $\Lambda$ -dependent contribution. The first part of the correction is shown by the shift in the curves for  $\Lambda=0$ , while the second part is closely equal to  $-0.15 \Lambda$  for the energies of interest here.

Figure 3 shows an energy-dependent discrepancy between theory and experiment which is somewhat outside the estimated errors from the Coulomb corrections. *A priori*, we prefer the theory including the corrections of Warburton and Gourdin and the over-all fit appears slightly better in this case. The best fit with the corrected theory, averaged over the three energies, is for  $\Lambda \approx 0.1$ . Including the uncertainty introduced by the Coulomb corrections, and assuming the theory to be not too much in error, the final result is

$$\Lambda = +0.1 \pm 0.3.$$

<sup>20</sup> A. E. A. Warburton and M. Gourdin, *Nuovo Cimento* **22**, 362 (1961).

The error estimate is dominated by the theoretical uncertainties, and can hardly be justified in detail.

A variety of previous estimates of  $\Lambda$  have been made, all for  $t_r=22.4 m_\pi^2$ , except where otherwise noted:  $\Lambda \sim +0.6$ , from  $\pi^0$  photoproduction<sup>21</sup>;  $-0.6 \leq \Lambda \leq 0.0$  from  $\pi^+$  and  $\pi^0$  photoproduction<sup>18</sup>;  $\Lambda \sim +1$  ( $t_r=16 m_\pi^2$ )<sup>4</sup> and  $\Lambda \approx +0.2^{20}$  from the energy dependence of  $R$  at  $90^\circ$  c.m.;  $\Lambda = -1.2 \pm 0.4^{22}$ ; and  $\Lambda = 0.7 \pm 0.7$ ,<sup>9</sup> from  $\pi^+$  photoproduction. The present determination appears to be more accurate and freer from theoretical uncertainties than previous ones. In particular, when evaluating  $\Lambda$  from  $\pi^+$  or  $\pi^0$  photoproduction, the uncertainties in the isovector amplitudes introduce much more serious problems than here.

The only previous estimate of  $\Lambda$  which is inconsistent with ours is that of Robinson *et al.*<sup>22</sup> This disagreement has been discussed previously in a brief report of this experiment.<sup>23</sup> They have found  $\Lambda = -1.2 \pm 0.4$  by comparing the McKinley theory (without the correction of Warburton and Gourdin) with  $\pi^+$  photoproduction, mainly at backward angles at photon energies of 220 to 250 MeV. From the dashed curves of Fig. 3, it is apparent that a comparison of  $R$  with this theory leads to a quite different estimate of  $\Lambda$ . We believe that the most plausible explanation of the discrepancy is that there is a sizeable error in the theoretical evaluation of the isovector amplitude.

#### ACKNOWLEDGMENTS

We are especially grateful to Dr. F. F. Liu for making available to us his evaluations of the McKinley theory. We would like to thank Lynn Boyer and John Grant for their help with the experimental apparatus. We would also like to acknowledge helpful conversations with Dr. A. E. A. Warburton and Professor G. Feldman, Professor P. T. Matthews, and Professor M. Gourdin.

<sup>21</sup> B. De Tollis and A. Verganelakis, *Nuovo Cimento* **22**, 406 (1961).

<sup>22</sup> P. M. Baum and C. S. Robinson, Physics Department, University of Illinois, Tech. Rept. No. 40, 1962 (unpublished); C. S. Robinson, P. M. Baum, L. Criegee, and J. M. McKinley, *Phys. Rev. Letters* **9**, 349 (1962).

<sup>23</sup> J. Pine and M. Bazin, *Phys. Letters* **5**, 168 (1963).